Molecular Catalysis 474 (2019) 110420

Contents lists available at ScienceDirect

Molecular Catalysis

journal homepage: www.elsevier.com/locate/mcat

Batch versus flow stereoselective hydrogenation of α-acetamido-cinnamic acid catalyzed by an Au(I) complex

Alina Negoi[a], Bogdan Cojocaru[a], Vasile I. Parvulescu[a,*], Nora Imlyhen[b], Maryse Gouygou[b,*]

[a] Department of Organic Chemistry, Biochemistry and Catalysis, Faculty of Chemistry, University of Bucharest, Bd. Regina Elisabeta no. 4–12, 030018 Bucharest 030016, Romania

[b] CNRS, LCC (Laboratoire de Chimie de Coordination), Universite de Toulouse, UPS, 205, route de Narbonne, 31077 Toulouse, France

ARTICLE INFO

Keywords:
Au(I) *(2S,4S)*-1-*tert*-butoxycarbonyl-4-diphenylphosphino-2-(diphenylphosphino-methyl) pyrrolidine (BPPM) complex
Stereoselective hydrogenation of α-acetamidocinnamic acid to the (*R*)-N-acetyl-phenylalanine
Heterogenization of the Au-BPPM catalyst onto a CNT support
Flow stereo-hydrogenation

ABSTRACT

A chiral gold (I) *(2S,4S)*-1-*tert*-butoxycarbonyl-4-diphenylphosphino-2-(diphenylphosphino- methyl) pyrrolidine (BPPM) complex has been prepared using [Au(SMe_2)Cl] as precursor. The heterogenization of the Au-BPPM catalyst onto the CNT support followed two routes, ie (i) the non-covalent immobilization of the gold(I)complex by dry-impregnation, and (b) covalent immobilization of the gold(I)complex on a pre-functionalized CNT. These catalysts afford the stereoselective hydrogenation of α-acetamidocinnamic acid to the (*R*)-N-acetyl-phenylalanine enantiomer. The nature of the solvent affected both the enantioselectivity and TOFs. Among MeOH, EtOH, and TFE, methanol appeared to be the most efficient one (at 80 °C a TOF of 0.37 h^{-1} for a total enantioselectivity to the *R*-isomer). Transferring the reaction in the flow reactor, under similar conditions (methanol, room temperature) led to a 10 time increase of the TOF with no change in the stereoselectivity. The decrease of the TOF in time for both the reference Rh and the Au catalysts was assigned to their partial modification under the reaction conditions. The heterogenization of the Au-BPPM catalyst onto the CNT support, for the same content of Au-complex, led to a very important increase of the conversion with no change in the selectivity. However, the covalent bonding was more efficient affording a very high increase of the conversion even at room temperature (95% after 24 h), thus demonstrating that the anchoring a support increases the dispersion, and in consequence the efficiency. These CNT-Au-BPPM catalysts preserved the catalytic performances during recycling as also confirmed by the characterization results.

1. Introduction

Gold (I) complexes have received considerable attention in the field of organic synthetic chemistry owing to their capability to catalyze a broad panel of transformations [1–4]. They are the most effective catalysts for the electrophilic activation of alkynes under homogeneous conditions, and a broad range of versatile synthetic tools have been developed for the construction of carbon–carbon or carbon–heteroatom bonds. The majority of gold (I) complexes employed as catalyst precursors are phosphine complexes or N-heterocyclic carbene complexes of the type [AuClL].

The development of efficient asymmetric transformations with chiral gold catalysts was challenging given the intrinsic structural characteristics of the gold (I) complexes. Because of their linear geometry, the chiral ligand (L *) and the substrate are on the opposite side to the metal center. As a result, the substrate is easily displaced from the chiral pocket.

However, three main systems have been successfully implemented in the development of homogeneous gold-catalyzed enantioselective reactions [5]. Chiral monodentate phosphine-type ligands were first used in gold-catalysis asymmetric reactions. Examples were reported early in 1986 by Ito et al for the enantio- and diastereoselective synthesis of a 5-alkyl-2-oxazoline-4-carboxylate via aldol reaction between isocyanoacetate and benzaldehyde [6]. Then, various phosphine–ligated gold(I) complexes have been designed for enantioselective gold catalysis [5]. However one of the most widely used strategies is the use of bimetallic gold complexes in particular with atrop-isomeric diphosphines ligands. Diphosphine–ligated gold(I) complexes enable various asymmetric transformations such as enantioselective alkyne, allenes and alkenes activation and enantioselective transformation of diazo compounds [5]. The use of chiral counter-anions to achiral cationic gold(I) catalysts has emerged as an alternative strategy as initially demonstrated in the intramolecular hydroamination and hydroalkoxylation reaction of allenes with high asymmetric induction

* Corresponding authors.
E-mail addresses: parvulescu@g.unibuc.ro (V.I. Parvulescu), maryse.gouygou@lcc-toulouse.fr (M. Gouygou).

https://doi.org/10.1016/j.mcat.2019.110420
Received 12 March 2019; Received in revised form 23 April 2019; Accepted 20 May 2019

[7–10].

In contrast, little work has been done on enantioselective hydrogenation catalyzed by gold(I). In 2005, Corma and co-workers reported the first gold (I) catalyst, a dimeric gold(I) complex bearing the [(*R,R*)-Me-Duphos] diphosphine ligand, able to perform enantioselective hydrogenation of alkenes and imines with high catalytic activities and selectivities under mild reaction conditions [11]. The reaction mechanism studied by density functional theory calculations revealed an ionic hydrogenation [12]. Other examples reported by the Corma's group refer to the hydrogenation of prochiral alkenes catalyzed by a bis N-heterocyclic gold (I) complex [13].

Heterogeneous stereoselective hydrogenation has also been carried with gold (III) complexes. Thus, studies carried out with Au(III) − Schiff base complexes in combination with kinetic experiments and theoretical calculations shown that the nature of the solid support (polarity and proton-donating ability) is important in this reaction. As an effect, the activity of these catalysts may be enhanced by a simple grafting of these complexes onto selected surfaces [14].

As part of our continuing interest in homogeneous gold catalysis [15] and in heterogeneous enantioselective hydrogenation [16] we report herein the preparation of chiral gold catalysts (Fig. 1), and their application in enantioselective hydrogenation. The aim of this study was to compare the behavior of a gold complex as a homogeneous or heterogeneized catalyst (resulted either via non-covalent or covalent linkage onto carbon nanotubes) in both batch and flow conditions.

2. Experimental

Unless otherwise stated, all syntheses were run under Argon using Schlenk techniques. All reagents: (*2S,4S*)-1-tert-butoxycarbonyl-4-diphenylphosphino-2-(diphenylphosphino- methyl) pyrrolidine (BPPM), [Au(SMe_2)Cl], α-acetamidocinnamic acid (ACA), 98% purity, and methyl-3-aminobutanoate (MAB), carbon nanotube (CNT), were purchased from Sigma-Aldrich and used as received without further purification. Dichloromethane and pentane were dried under N_2 using a solvent purification system (SPS). Methanol (MeOH, 99.8% purity), ethanol (MeOH, 96% purity), TFE (2,2,2-trifluoroethanol, 99.5% purity) were purchased from Sigma-Aldrich. The (*R, R*)-MeDuPhos-Rh complex was purchased from STREM Chemicals, Inc.

NMR spectra were recorded at 25 °C on Advance 400 Ultrashield and Advance III Ultrashield Plus 500 MHz Bruker apparatus. ^{1}H NMR, ^{13}C{^{1}H} NMR chemical shifts are referenced to the solvent signal. ^{31}P{^{1}H} NMR chemical shifts are referenced to an external standard (85% aqueous H_3PO_4). Multiplicity is indicated as follows: s = singlet, bs = broad singulet, d = doublet, m = multiplet. ESI analyses were performed on a UPLC Xevo G2 Q TOF spectrometer.

2.1. Synthesis of the gold(I) complex, Au-BPPM

2.1.1. Non-covalent immobilization of the gold(I)complex onto CNT

The heterogeneous 4 wt% complex **CNT@Au-BPPM** (CNT-carbon nanotube) has been prepared by dry-impregnation of the resulted complex. For this purpose, the calculated amount of the **Au-BPPM** was dispersed in methanol and the solution was added drop-by-drop to the CNT (Sigma-Aldrich) at dry. Then, the catalysts were treated under vacuum at room temperature for 8 h.

2.1.2. Covalent immobilization of the gold(I)complex onto CNT, CNT-Au-BPPM

(2S,4S)-BPPM grafted on CNT was prepared according to a previously reported procedure [17]. (Scheme 2) The concentration of the grafted ligand was calculated to afford a 4 wt% Au loading after the complexation. Then the complexation with [Au(SMe_2)Cl] followed the same protocol with that described above (Scheme 1). The ICP-OES analysis confirmed the loading of Au (3.92 wt%).

2.1.3. Catalyst characterization

The investigated catalysts were characterized by ATR-FTIR, Raman and DR-UV–vis spectroscopy. Attenuated total reflection Fourier transformed infrared (ATR-FTIR) spectra were recorded using a PerkinElmer Spectrum Two spectrometer having an ATR cell equipped with a diamond plate (Pike Technologies, Madison, WI). The spectra were recorded with a 4 cm^{-1} resolution at 20 scans. Raman spectra were acquired in the extended spectral region from 150 up 4000 cm^{-1} with a Horiba JobinYvon - Labram HR UV–vis-NIR Raman Microscope Spectrometer (˜0.4 µm resolution on X and Y axes and ˜0.7 µm resolution on Z axe), at 488 nm and 633 nm. Diffuse reflectance UV–vis measurements were carried out with a Thermo Electron Specord 250 using an integrating sphere and MgO as reference. The slit was set at 4 nm. The spectra of the catalysts were recorded in reflectance units and were transformed in Kubelka–Munk remission function F(R).

2.2. Catalytic reactions

Hydrogenation of ACA to (*R*)-N-acetyl-phenylalanine and of MAB has been carried out in batch and flow reactors, respectively. Batch reactions were carried out in a stainless steel pressure autoclave from Parr (50 mL) using 80 mg ACA, 10 mg catalyst, and 25 mL MeOH, EtOH or TFE. After closing, the autoclave was purged three times with nitrogen and then pressurized at 40 atm H_2. The mixture was then vigorously stirred (1.000 rpm) for 24 h at temperatures in the range rt-80 °C.

Flow reactions were carried out in a tubular stainless-steel microreactor system (length of 300 mm and i.d. of 9 mm, equipped with a thermocouple in the middle) from PID&ENG at a pressure of 40 atm H_2. 80 mg ACA and 10 mg catalyst were dispersed in methanol in a volume filling of the entire system (around 60 mL). The microreactor was placed inside a ceramic resistance furnace where the temperature control was achieved with a TohoTTM-204 controller (K-type thermocouple at the middle-level of the ceramic jacket) and an Elko ELK-38 indicator (K-type thermo-couple in contact with the microreactor body). Both instruments (calibrated against a high temperature glass thermometer) were computer interfaced through RS-232 to TTL level converters based on Maxim MAX-232 IC allowing bidirectional Modbus communication. The flow control (10 mL min^{-1}) was performed for the liquid phase by a pump (KnauerK-501 HPLC pump, computer controlled by RS-232 serial interface). The liquid output from the reactor was collected into an open glass vessel. Samples were extracted from

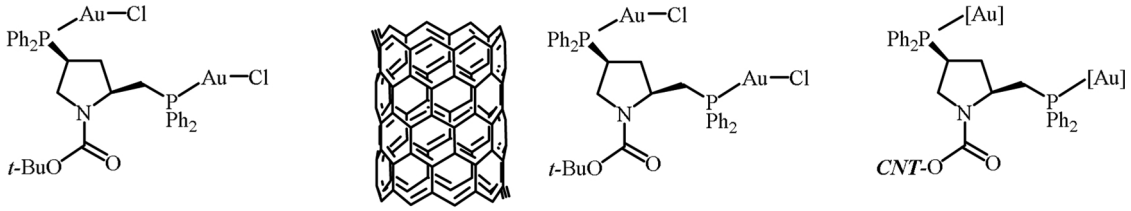

Au-BPPM **CNT@Au-BPPM** **CNT-Au-BPPM**

Fig. 1. Gold (I) complexes used in this work.

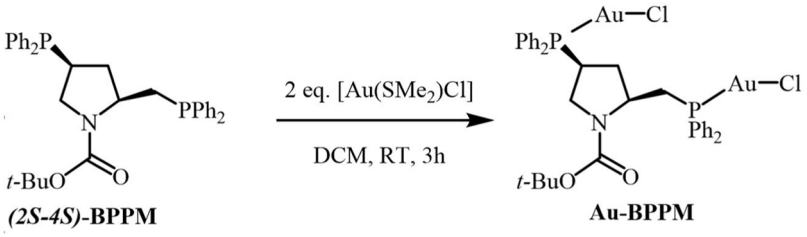

Scheme 1. Complexation of (*2S,4S*)-BPPM with [Au(SMe_2)Cl].

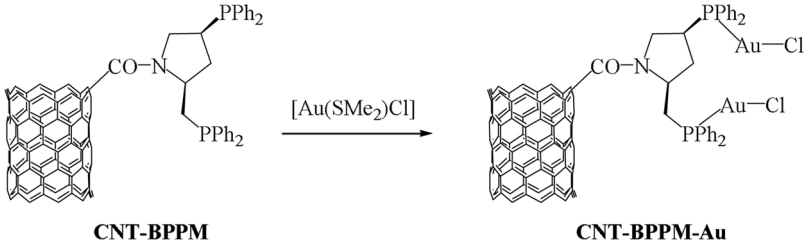

Scheme 2. Complexation of (*2S,4S*)-BPPM grafted on CNT with [Au(SMe_2)Cl].

the collector vessel with the peristaltic pump P2 (HeidolphPD 5001, computer controlled through a parallel port relay inter-face) and dispensed in individual glass tubes (covered with small funnels to reduce evaporation) by the help of a fraction collector (Teledyne ISCO Foxy Jr, computer connected by RS-232 serial link). The operational parameters of the installation (temperature, liquid flow rate, collection of samples) were controlled by a code developed in C-programming language running on GNU/Linux operating system (32-bit CentOS 6).

2.3. Analysis of the reaction products

Quantitative analysis of the reaction products was performed using a high performance liquid chromatography coupled with fluorescent and diode array detection (HPLC-FLD/DAD) method. The analyses were carried out with an Agilent 1260 modular system equipped with CHIRALPAK QD-AX column (150 × 4.6 mm ID, 5 µm). Working parameters of the HPLC-FLD/DAD system were: injection volume of 20 µL, mobile phase composition: MeOH:CH_3COOH:CH_3COONH_4 = 98:2:0.5, flow rate of 1.0 mL/min, temperature of the column 25 °C, 338 nm and 262 nm for OPA and FMOC derivatives, respectively. FLD was set up at 340 nm extinction wavelength and 450 emission wave-length. Before analysis, the amino-compounds were derivatized using OPA and FMOC reagents for primary and secondary amino groups, respectively. Finally, 200 µL sample were mixed with 200 µL derivatization agent and diluted in 1 mL borate buffer.

The borate buffer solution contained 0.4 mol $Na_2[B_4O_5(OH)_4]$ in 1 L of distilled water. The pH value was adjusted to 10.2 by boric acid. The OPA (*o*-phthalaldehyde) solution was prepared by adding 10 mg OPA in 1 mL 0.4 M borate buffer. FMOC (9-fluorenylmethyl chloroformate) solution contained 2.5 mg FMOC in 1 mL acetonitrile.

α-acetamidocinnamic acid

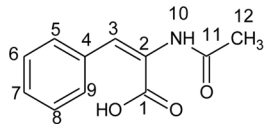

^{1}H-NMR (500.13 MHz, DMSO-d6, δ ppm, J Hz): 12.60 (s, 1H, -COO**H**), 9.45 (s, 1H, H-10, -N**H**), 7.62-7.37 (m, 5H, H-5, H-6, H-7, H-8 and H-9), 7.23 (s, 1H, H-3), 1.99 (s, 3H, H-12).**^{13}C-NMR** (125.77 MHz, DMSO-d6, δ ppm): 169.2 (C-1), 166.4 (C-11), 133.7 (C-3), 131.1 (C-4), 129.7 (C-5 and C-9), 129.1 (C-7), 128.5 (C-6 and C-8), 127.3 (C-2), 22.4 (C-9).

(*R*)-N-acetyl-phenylalanine

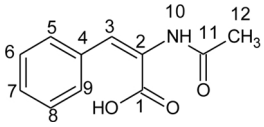

^{1}H-NMR: (500.13 MHz, DMSO-d6, δ ppm, J Hz): 12.70 (s, 1H, -COO**H**), 8.21 (s, 1H, H-10, -N**H**), 7.28-7.21 (m, 5H, H-5, H-6, H-7, H-8 and H-9), 4.42 (m, 1H, H-2, J^A= 5.0 Hz, J^B = 3.1 Hz), 3.07-2.81 (m, 2H, H-3, J^A=5.0 Hz, J^B=8.9 Hz), 1.79 (s, 3H, H-12); **^{13}C-NMR**: (125.77 MHz, DMSO-d6, δ ppm): 173.1 (C-1), 169.2 (C-11), 137.6 (C-4), 129.0 (C-5 and C-9), 128.1 (C-6 and C-8), 126.3 (C-7), 53.4 (C-2), 36.7 (C-3), 22.2 (C-12).

3. Results and discussions

3.1. Catalysts characterization

The ATR-FTIR spectrum of Au-BPPM (Fig. 2) contains typical bands of this complex, ie bands assigned to the vibrations of the C—H skeletal (1229, 1259 cm^{-1}), C—H deformation of the C—CO out-of-plane deformation (412 cm^{-1}), C–H scissor (1482 cm^{-1}), asymmetric C—H stretching (2861 and 2972 cm^{-1}), C—N—C deformation (421, 432, 439, 457 1347, 1359 and 1394 cm^{-1}), C—C=O in-plane deformation (474, 489, 618 cm^{-1}), C—C skeletal (499, 515, 521, 545, 584 815, 855, 906, and 929 cm^{-1}), C—O—C deformation (691, 810 cm^{-1}), C—N stretching

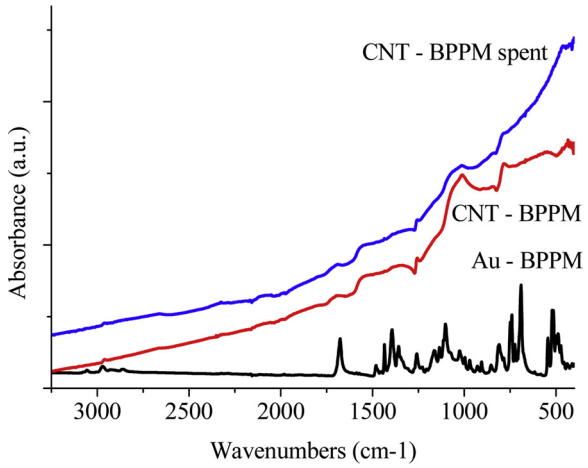

Fig. 2. ATR-FTIR spectra of Au-BPPM, CNT@Au-BPPM and spent CNT@Au-BPPM catalysts.

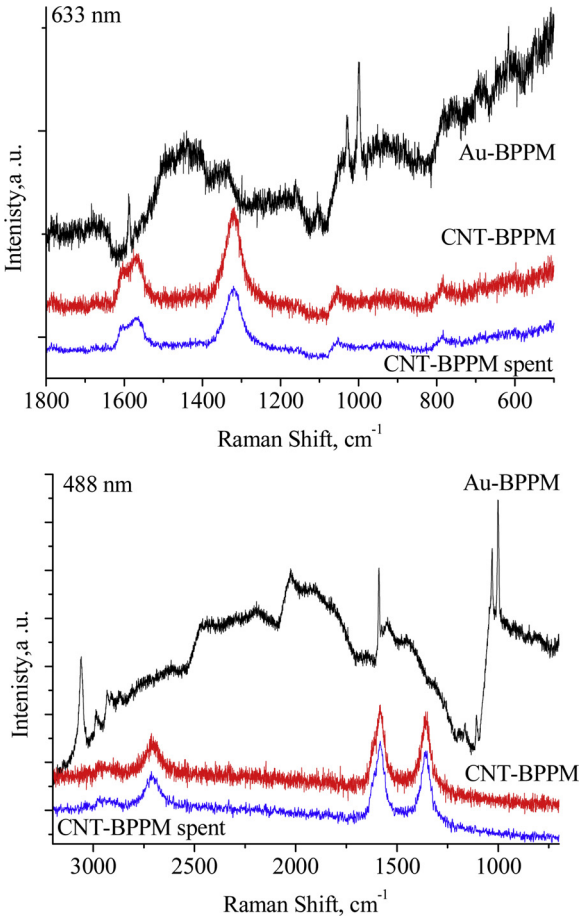

Fig. 3. Raman spectra of Au-BPPM, CNT@Au-BPPM and spent CNT@Au-BPPM catalysts.

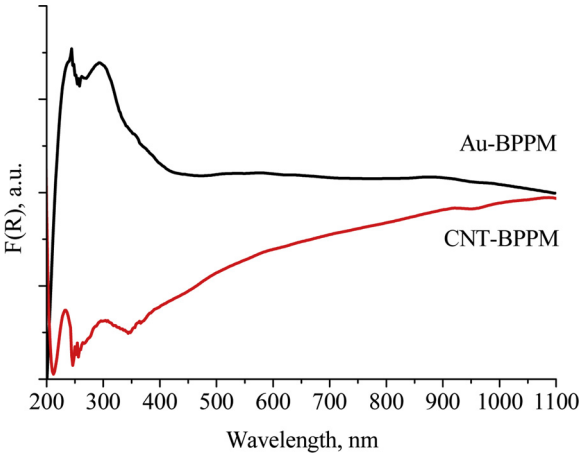

Fig. 4. DR-UV–vis spectra of Au-BPPM, CNT@Au-BPPM and spent CNT@Au-BPPM catalysts.

(1164, 1207 and 1273 cm^{-1}), P—C stretching (712, 725, 741, 750 and 785 cm^{-1}), P-N-C asymmetric stretching (958, 971, 997, 1025, 1075 and 1103 cm^{-1}), P-Ph stretching (1113, 1136 and 1455 cm^{-1}), P-Ph ring in-plane stretching (1113, 1136 and 1455 cm^{-1}), amide N—H deformation (1588 cm^{-1}), amide C=O stretching (1677 cm^{-1}), and amide N—H stretching (3057 and 3075 cm^{-1}) bonds. The immobilization of the complex (CNT@Au-BPPM spectrum) led to both a shift and diminution of the intensity of these bands. Accordingly, only the bands assigned to the vibrations of the C—C=O in-plane deformation (474 cm^{-1}), P—C stretching (784 cm^{-1}), C—C skeletal (850 cm^{-1}), P-N-C asymmetric stretching (1010 cm^{-1}), C—H skeletal (1258 cm^{-1}), C—N—C deformation (1352 cm^{-1}) and asymmetric C—H stretching (2960 cm^{-1}) respectively were detected in this spectrum. Further, the spectrum collected for the spent CNT@Au-BPPM shown no other changes in the intensity or location of the bands compared to fresh CNT@Au-BPPM.

Raman spectra were collected for Au-BPPM, CNT@Au-BPPM and spent CNT@Au-BPPM catalysts are presented in Fig. 3. Considering both irradiation sources (488 and 633 nm respectively), the spectrum of Au-BPPM contains lines assigned to vibrations of the C—C alicyclic and aliphatic chain at 760, 783, 998, 1030, 1104, 1160 and 1230 cm^{-1}, the asymmetric CH_2 at 1410 and 1143 cm^{-1}, and the C—C aromatic ring at 1587 cm^{-1}. The immobilization of the Au-BPPM caused both a reduction of the intensity of these lines and a shift. Thus, the lines assigned to vibrations of the C—C alicyclic and aliphatic chain shifted at 1053 and 1157 cm^{-1}, and that of the C—C aromatic ring at 1570 cm^{-1}. Like for the ATR-FTIR spectra the spectrum collected for the spent CNT@Au-BPPM shown no other changes in the intensity or location of the bands compared to fresh CNT@Au-BPPM. Supplementary, fresh CNT@Au-BPPM and spent CNT@Au-BPPM shows the typical Raman shifts of the D, G and G' bands at 1322, 1570 and 2716 cm^{-1} respectively.

Fig. 4 shows the DR-UV–vis spectra of Au-BPPM, CNT@Au-BPPM and spent CNT@Au-BPPM catalysts. An absorption band at ~230 nm is characteristic to Au ions, while the band at about 290 nm is characteristic to symmetry-allowed p_{σ}-d_{σ^*} transition in binuclear gold complexes [18].

Table 1
Catalytic results for the hydrogenation of α-acetamidocinnamic acid to (*R*)-N-acetyl-phenylalanine with (*R, R*)-Rh-MeDuPhos under batch homogeneous conditions (24 h).

Entry	Time, min	Conversion (%)	Selectivity (%)	Ee(%)	TON	TOF (h^{-1})
1	30	28	100	> 99 (*R*)	6.6	13.2
2	90	58	100	85 (*R*)	13.6	9.1
3	180	79	100	80 (*R*)	21.0	7.0
4	360	100	100	75 (*R*)	23.5	5.6

Reactions conditions: 0.05 g ACA, 0.005 g of Rh-complex, 40 atm H_2; 25 mL methanol, room temperature.

3.2. Hydrogenation of α-acetamidocinnamic acid to (R)-N-acetyl-phenylalanine under batch homogeneous catalytic conditions

Scheme 3 In the first set of experiments, the catalytic performances of the new synthesized Au-complex catalyst, Au-BPPM, were compared to those of the (*R, R*)-MeDuPhos-Rh complex under batch homogeneous catalytic conditions. Indeed, Rh-chiral diphosphine based catalysts are the most successful ligands developed for the asymmetric hydrogenation of C=C bonds such as unsaturated prochiral acids [19]. Particularly, the Rh-DuPhos catalysts show excellent enantioselectivies (up to 98% ee) for the asymmetric hydrogenation of dehydroamino acid derivates [19,20]. In this study, to evaluate the catalytic performance of

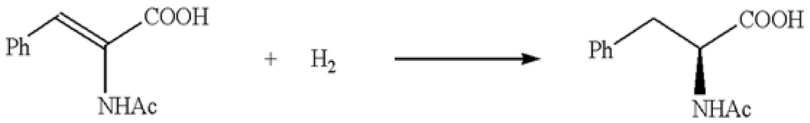

Scheme 3. Hydrogenation of α-acetamidocinnamic acid to (*R*)-N-acetyl-phenylalanine.

Table 2
Catalytic results for the hydrogenation of α-acetamidocinnamic acid to (R)-N-acetyl-phenylalanine with Au-BPPM catalyst under batch homogeneous conditions (24 h).

Entry	Solvent	Temperature (°C)	Conversion (%)	Selectivity (%)	Ee (%)	TON	TOF (h^{-1})
1	MeOH	RT	10.8	100	> 99 (*R*)	2.5	0.10
2	MeOH	80	27.1	100	> 99 (*R*)	8.8	0.37
3	EtOH	RT	7.2	100	> 99 (*R*)	2.3	0.10
4	TFE	RT	3.2	100	98 (*R*)	1.0	0.04

Reactions conditions: 0.08 g ACA, 0.01 g of Au-complex, 40 atm H_2; 25 mL solvent, room temperature.

Table 3
Catalytic results for the hydrogenation of α-acetamidocinnamic acid to (*R*)-N-acetyl-phenylalanine under flow homogeneous catalytic conditions onto the **Au-BPPM** catalyst.

Entry	Temperature (°C)	Time h	Conversion (%)	Selectivity (%)	Ee (%)	TON	TOF (h^{-1})
1	RT	0.5	1.2	100	> 99 (*R*)	0.39	0.78
2		1	4.6	100	> 99 (*R*)	1.49	1.49
3		3	10.7	100	> 99 (*R*)	3.48	1.16
4		5	14.6	100	> 99 (*R*)	4.74	0.95
5		8	16.8	100	> 99 (*R*)	5.46	0.68
6	80	0.5	4.8	100	> 99 (*R*)	1.56	3.12
7		1	16.3	100	> 99 (*R*)	5.29	5.29
8		3	36.2	100	> 99 (*R*)	11.76	3.92
9		5	46.2	100	> 99 (*R*)	15.01	3.00
10		8	56.1	100	> 99 (*R*)	18.23	2.28

Reactions conditions: 0.08 g ACA, 0.01 g of Au-complex, 40 atm H_2; 25 mL methanol.

Table 4
Catalytic results for the hydrogenation of *α*-acetamidocinnamic acid to (*R*)-phenylalanine with immobilized Au-catalysts.

Entry	Catalyst	Temperature (°C)	Time (h)	Conversion (%)	Selectivity (%)	ee (%)
1	CNT@Au-BPPM[a] 4 wt%	80	2	17	100	83 (*R*)
2	CNT@Au-BPPM[a] 4 wt%	80	24	69	100	71 (*R*)
3	CNT@Au-BPPM [a] 4 wt%	80	48	72	100	63 (*R*)
4	CNT-Au-BPPM [a] 4 wt%Au	RT	2	21	100	85 (*R*)
5	CNT-Au-BPPM[a] 4 wt%Au	RT	24	95	100	70 (*R*)
6	CNT-Au-BPPM[a] 4 wt%Au	RT	48	96	100	71 (*R*)
7	CNT-Au-BPPM[b] 4 wt%Au	RT	2	57	100	98(*R*)

Reaction conditions: 0.05 g ACA, 0.005 g of Au-complex, 40 atm H_2, methanol.
[a] Batch conditions.
[b] Flow conditions.

the Au-BPPM catalyst, α-acetamidocinnamic acid has been selected as a model substrate.

Tables 1 and 2 compile catalytic results using (*R, R*)-MeDuPhos-Rh and the new synthesized Au-complex catalyst. The experiments carried out with Rh confirmed the total stereoselectivity to the (*R*) isomer, but only for small reaction times (ie 30 min), that correspond to conversions below 30% (Table 1, entry 1). An increase of the reaction time led to an increase of the conversion reaching 100% after 6 h (Table 1, entry 4) but with a progressive decrease of the enantioselectivity. The calculated values of TON and TOF reflect this behavior. Thus, the evolution of the TOF in time reflects a deactivation of the catalysts [21] that may correspond to a partial degradation of the complex leaving a less complexed metal.

Working with Au-complex catalyst in the same catalytic conditions, the reaction was much slowly compared to Rh catalysts. As expected the increase of the temperature led to an increase of the conversion. However, the enantioselectivity is better than for Rh-MeDuPhos, demonstrating an increased stability of the Au-complex. It has been preserved at almost total even after the increase of the temperature at 80 °C (Table 2, entries 1–2). The higher TON was nearby 9 at 80 °C after 24 h that corresponded to TOFs smaller than 0.5. The solvent has also an influence on this reaction. While for methanol and ethanol the performances were quite similar (Table 2, entry 1 *vs* entry 3), working in TFE led to a decrease in both the conversion and the enantioselectivity. A negative influence of TFE in asymmetric reactions has also been previously reported in the literature [22].

3.3. Hydrogenation of α-acetamidocinnamic acid to (R)-N-acetyl-phenylalanine under catalytic flow homogeneous conditions

The hydrogenation of α-acetamidocinnamic acid to (*R*)-N-acetyl-phenylalanine under catalytic flow homogeneous conditions has been carried out in methanol as solvent at room temperature and at 80 °C taking as reference the results collected from the reactions carried out in batch. In all experiments, excellent chemo- and enantioselectivies were obtained. The increase of the reaction time affords an increased conversion irrespective of the temperature (room temperature, Table 3, entries 1–5, and 80 °C, Table 3, entries 6–10). Very important, these

increases were produced with no change in the chemo- or enantioselectivity. However, the values of TOFs also shown a depletion for reaction times longer than 3 h that may also suggest a kind of deactivation. Since the enantioselectivity has not changed this decrease could be simply assigned to a more advanced strong chemisorption of either the substrate or the product onto the Au-BPPM catalyst. This process in favored by the increase of the temperature (Table 3, see RT versus 80 °C).

3.4. Hydrogenation of α-acetamidocinnamic acid to (R)N-acetyl-phenylalanine with the immobilized Au-BPPM catalysts

Table 4 shows the catalytic results with the two immobilized Au catalysts, CNT@Au-BPPM and CNT-Au-BPPM. The conversions were higher than those measured for Au-BPPM under flow conditions but the enantioselectivities were inferior (63–83 % ee). The increase of the reaction time affords an increased conversion with the prize of a decrease in the enantioselectivity (Table 4 entries 1–3). This decrease is the effect of both non-covalent (CNT@Au-BPPM) and covalent (CNT-Au-BPPM) immobilization of the Au-BPPM complex. Most probably, for CNT@Au-BPPM this interaction occurs via a $\pi-\pi$ stacking interaction between the aromatic entities of the ligand and CNT. For the second case, the decrease of the enantioselectivity is the effect of the rigidity induced by the anchoring (Scheme 2). In both cases, a change in the bite-angle of complex could be responsible for this decrease. On the other hand, the high dispersion provided by the covalent immobilization of the gold(I)complex onto CNT produces an enhanced availability to the complex and, thus, an increased conversion compared to the impregnated gold complex (Table 4 entries 4–6 *vs* entries 1–3). Recycling the CNT-Au-BPPM catalysts for five times occurred with no change in the catalytic performances thus confirming the characterization results.

Finally, the gold(I) complex covalently immobilized onto CNT, CNT-Au-BPPM, was evaluated under catalytic flow conditions (Table 4, entry 7). Under the experimental conditions (at 25 °C, for 2 h), the product could be continuously produced with a 57% conversion and an excellent enantioselectivity of 98%.

4. Conclusions

In conclusion, this study demonstrated the capability of the Au-BPPM catalyst to afford the stereoselective hydrogenation of α-acetamidocinnamic acid to the (*R*)-N-acetyl-phenylalanine enantiomer. The nature of the solvent affected both the enantioselectivity and TOFs. In the investigated series (MeOH, EtOH, TFE) methanol appeared to be the most efficient one (at 80 °C a TOF of 0.37 h^{-1} for a total enantioselctivity to the *R*-isomer). Using the reference (*R, R*)-Rh-MeDuPhos, the enantioselctivity to the *R*-isomer was total only at room temperature, however with a TOF fifty times higher. Transferring the reaction in the flow reactor, under similar conditions (methanol, temperature) led to a 10 time increase of the TOF of the Au-BPPM catalyst with no change in the stereoselectivity. The decrease of the TOF in time for both the reference Rh and the Au catalysts was assigned to their partial modification in the reaction conditions.

The heterogenization of the Au-BPPM catalyst onto the CNT support, for the same content of Au-complex, led to a very important increase of the conversion with no change in the selectivity. However, the covalent bonding was more efficient affording a very high increase of the conversion even at room temperature (95% after 24 h). The anchoring onto the support increased the dispersion, and in consequence the efficiency. However, under batch conditions, for both catalysts, the enantioselectivity suffered an important depletion (70% in *R*). But, transferring the covalent bonded CNT-Au-BPPM catalyst in the flow reactor corresponded to an excellent ee (98%) for an acceptable conversion. Furthermore, recycling the CNT-Au-BPPM catalysts occurred with no change in the catalytic performances as also confirmed by the characterization results.

References

[1] A. Corma, A. Leyva-Pérez, M.J. Sabater, Chem. Rev. 111 (2011) 1657–1712.
[2] R. Dorel, A.M. Echavarren, Chem. Rev. 115 (2015) 9028–9072.
[3] D. Pflästerer, A.S.K. Hashmi, Chem. Soc. Rev. 45 (2016) 1331–1367.
[4] Y. Li, W. Li, J. Zhang, Chem. Eur. J. 23 (2017) 467–512.
[5] W. Zi, F.D. Toste, Chem. Soc. Rev. 45 (2016) 4567–4589 and the references cited therein.
[6] Y. Ito, M. Sawamura, T. Hayashi, J. Am. Chem. Soc. 108 (1986) 6405–6406.
[7] R.A. Widenhoefer, Chem. Eur. J. 14 (2008) 5382–5391.
[8] S. Sengupta, X. Shi, ChemCatChem 2 (2010) 609–619.
[9] A. Pradal, P.Y. Toullec, V. Michelet, Synthesis (2011) 1501–1514.
[10] Y.-M. Wang, A.D. Lackner, F.D. Toste, Acc. Chem. Res. 47 (2014) 889–901.
[11] C. Gonzalez-Arellano, A. Corma, M. Iglesias, F. Sanchez, Chem. Commun. (2005) 3451–3453.
[12] A. Comas-Vives, G. Ujaque, J. Am. Chem. Soc. 135 (2013) 1295–1305.
[13] A. Arnanz, C. Gonzalez-Arellano, A. Juan, G. Villaverde, A. Corma, M. Iglesias, F. Sanchez, Chem. Commun. (2010) 3001–3003.
[14] A. Comas-Vives, C. Gonzalez-Arellano, A. Corma, M. Iglesias, F. Sanchez, G.J. Ujaque, J. Am. Chem. Soc. 128 (2006) 4756–4765.
[15] K. Fourmy, S. Mallet-Ladeira, O. Dechy-Cabaret, M. Gouygou, Organometallics 32 (2013) 1571–1574.
[16] C.C. Gheorghiu, B.F. Machado, C. Salinas-Martínez de Lecea, M. Gouygou, M.C. Román-Martínez, P. Serp, Dalton Trans. 43 (2014) 7455–7463.
[17] T.P. Dang, H.B. Kagan, Chem. Commun. (1971) 481.
[18] D.M. Roundhill, J.P. Fackler Jr., Optoelectronic Properties of Inorganic Compounds, Springer Science & Business Media, 2013, p. 197.
[19] M.J. Burk, J.E. Feaster, W.A. Nugent, R.L. Harlow, J. Am. Chem. Soc. 115 (1993) 10125–10138.
[20] M.J. Burk, M.F. Gross, J.P. Martinez, J. Am. Chem. Soc. 117 (1995) 9375–9376.
[21] S. Kozuch, J.M.L. Martin, ACS Catal. 2 (2012) 2787–2794.
[22] N. Fleury-Bregeot, V. de la Fuente, S. Castillon, C. Claver, ChemCatChem 2 (2010) 1346–1371.